Hybrid Recurrent Neural Network for Drought Monitoring

Mengxue Zhang[1], **Miguel-Ángel Fernández-Torres**[1], **and Gustau Camps-Valls**[1]

[1]Image Processing Laboratory (IPL), Universitat de València

Abstract

Droughts are pervasive hydrometeorological phenomena and global hazards, whose frequency and intensity are expected to increase in the context of climate change. Drought monitoring is of paramount relevance. Here we propose a hybrid model for drought detection that integrates both climatic indices and data-driven models in a hybrid deep learning approach. We exploit time-series of multi-scale Standardized Precipitation Evapotranspiration Index together with precipitation and temperature as inputs. We introduce a dual-branch recurrent neural network with convolutional lateral connections for blending the data. Experimental and ablative results show that the proposed system outperforms both the considered drought index and purely data-driven deep learning models. Our results suggest the potential of hybrid models for drought monitoring and open the door to synergistic systems that learn from data and domain knowledge altogether.

1 Introduction

Droughts are one of the costliest natural disasters causing seriously destructive consequences on the ecological environment, agricultural production, and socio-economic impacts [1]. With global warming, the frequency of composite dry-heat events such as heatwaves and droughts has increased significantly. In these circumstances, advanced monitoring techniques are urgently required to effectively and rapidly detect droughts [2], as well as to ameliorate risk management [3].

Due to the complex physical, chemical, and biological processes involved in drought events, much effort has been devoted to developing climate indices and (mostly mechanistic) analytical tools. In general, drought indices have become standardized tools for objectively quantifying the characteristics of these episodes in terms of intensity, magnitude, duration, and spatial extent. Three widely-used indices are the Palmer Drought Severity Index (PDSI), which is based on a soil water balance equation [4]; the Standardized Precipitation Index (SPI), which is based on a precipitation probabilistic model [5]; and the Standardized Precipitation-Evapotranspiration Index (SPEI), which combines both approaches [6]. The run theory deploys a bridge between climate indices and drought characteristics analysis [7, 8]. Other indices based on comprehensive remote sensing data have been proposed, either related to vegetation greenness, such as Normalized Difference Vegetation Index (NDVI), Vegetation Condition Index (VCI), or to water-limitation principles, as the Precipitation Condition Index (PCI) [9] and the Standardized Moisture Anomaly Index (SZI) [10].

Alternatively, data-driven models directly learn from historical drought records taking Essential Climate Variables (ECVs) as inputs to estimate drought intensity [11]. Existing models include but are not limited to k-nearest neighbors [12], artificial neural networks [13], support vector regression [13] and random forest [14]. More recently, deep architectures have been successfully employed, such as deep feed-forward neural networks [15], long short-term memory-based models [16], and advanced convolutional neural networks [17].

Tackling Climate Change with Machine Learning: workshop at NeurIPS 2022.

The integration of data-driven and physical models captures attention and promises a new generation of models for the Earth Sciences [18]. The hybrid machine learning framework combines the flexibility and representation capability of machine learning approaches with the consistency of domain knowledge. Validated examples include precipitation forecasting [19], terrestrial evaporation [20], cloud detection [21], and biophysical parameter [22]. In this paper, we propose a Hybrid Recurrent Neural Network (HRNN) to synergistically combine deep learning models and climate indices for the first time toward drought monitoring. Our experimental results show that our HRNN outperforms both indices and data-driven models, supporting the potential of hybrid frameworks for drought monitoring.

2 Data

Essential Climate Variables & Climate Indices First, we select total precipitation and air temperature @2m, which are well-known ECVs correlated to droughts, from the re-gridded ERA5-Land ($0.083^\circ \times 0.083^\circ$, 8 km^2) data [23], covering the period from Jan 2003 to Dec 2018 with a temporal resolution of 8 days. Second, SPEIs computed at different temporal resolutions (from 1 to 6 months) are selected as the climate. SPEI measures drought severity by taking into account both intensity and duration, and also allows us identifying their corresponding onset and offset times. Besides, being based on a water balance equation and a precipitation probabilistic model, the index provides complementary information to the raw ECVs data. Last but not least, it is a multi-scalar index that enables the identification of different drought types. It should be noted that, for the sake of measuring the implicit expert knowledge gathered in the formulation of the index, potential evapotranspiration (PET) for the SPEIs is computed using an equation that only relies on the ECVs mentioned above [24], despite more accurate methods are available for this estimation.

Drought Events & Dataset Splits The EM-DAT is a global database on natural disasters containing information about the occurrence and effects of more than 21,000 disasters in the world, from 1900 to the present [25]. In this study, time-series data of six recorded drought cases in Russia, Italy, and Afghanistan, from 2003 to 2018, are chosen. Two drought events are considered for each country, over extended regions covering these three countries, during the study period, as can be seen in Table A1. The training-validation-test data splits ensure that each subset contains one drought event with no overlapping times between them (see Table 1).

Table 1: Training, validation, and test dataset splits for Russia, Italy, and Afghanistan regions

	Training	Validation	Test
Russia	Jan 2004−Jun 2010	Jul 2010−Dec 2011	Jan 2012−Dec 2013
Italy	Jul 2012−Dec 2016	Mar 2011−Jun 2012	Jan 2017−Dec 2018
Afghanistan	Jan 2003−Sep 2008	Oct 2008−Dec 2009	Jan 2010−Dec 2011

3 Methodology

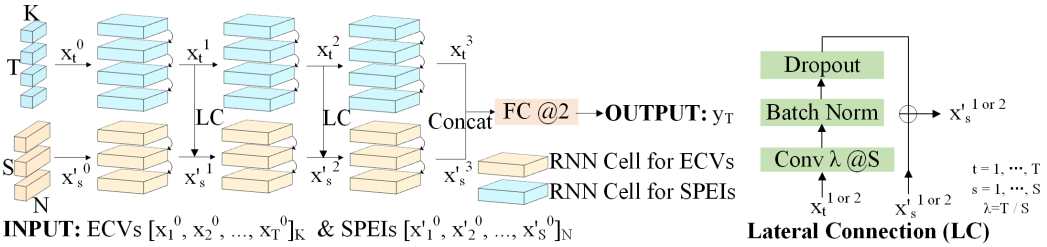

Figure 1: Graphical illustration of the proposed HRNN model for drought monitoring. The number after '@' is the dimension of the output features. Batch Norm, Conv, and FC in lateral connections (LC) represent batch normalization, 1D convolutional with a kernel size and a stride of λ, and fully connected layers, respectively.

Similar to [26], we tackle drought monitoring as a sequence binary classification task, i.e., for each spatial location and a given time step, our models make use of the time series including the last $T = 24$ steps ($\sim$ 6 months, according to [24]) of the $K = 2$ ECVs considered (precipitation and temperature) and blend the $S = 6$ time steps of the corresponding $N = 6$ SPEIs (computed from the same ECVs), in order to compute a probability score in [0, 1] to assess the drought severity.

Hybrid Recurrent Neural Network The scheme of the proposed HRNN is shown in Fig. 1, with lateral connections illustrated in detail on the right side. We integrate the physical knowledge in the HRNN by casting the SPEIs as complementary input features. To extract discriminative information about the droughts from both the ECVs and the SPEIs at different temporal resolutions, we design a dual-branch RNN instead of a single-branch multi-layer perceptron (MLP) or a single-branch RNN, with the aim of capturing their respective features at first. Then, inspired by [27], convolutional lateral connections are included to blend the ECVs into the SPEIs along the temporal dimension. Note that we consider the ECVs as supplementary to the SPEIs, instead of the opposite combination, since SPEIs encompass more persistent information, as demonstrated in Fig. A1. Finally, latent features are concatenated and fed into a fully connected layer with softmax activation to get the posterior probability of drought y_T.

Experimental Settings We mitigate the class imbalance (around 97% samples for non-drought event, demonstrated in Fig. A2) following an under-sampling strategy. Besides, all ECVs are standardized and truncated to the range $[-3, 3]$. We compare our HRNN to the SPEI-6 index, as well as to MLP, RNN, concatenated MLP (CMLP), and dual-branch RNN (DRNN) models. Specifically, the detection thresholds for the SPEI-6 are determined based on the best training F1-score. All models are implemented using PyTorch [28] and their hyperparameters are listed in Table A2. The network optimizer is set to Adam [29]. This setting is kept the same for three regions. Standard quantitative metrics are adopted for evaluation purposes: Macro F1-score, Precision-Recall (PR-AUC), and the Receiver Operating Characteristic AUC (ROC-AUC). The final test results are reported by averaging the outputs of 10 independent runs.

4 Experimental Results

Quantitative Results ROC-AUC scores for the different models can be found in Table 2, achieving the HRNN proposed the highest performance. AUC curves are depicted in Fig. 2. Other metrics are included in Table A3 and Fig. A3, where a few exceptions can be observed. For example, DRNN obtains a higher PR-AUC in Italy and CMLP achieves a higher F1 in Afghanistan; however, HRNN performs better overall for the three regions.

Qualitative Results Detection signals through time by computing the average drought score for all drought event spatial locations in each region are depicted in Fig. 3. We observe that HRNN has lower false alarms without reducing true positive rates. Besides, HRNN is able to capture the starting, ending, and duration of the drought events. We also noted that the predicted starting time is usually earlier than the one recorded in the EM-DAT, suggesting the drought warning capability of our approach. The monitoring maps and animations yielded by HRNN are shown in Fig. A4 and in the HRNN GitHub repo. It can be noticed a sparse and changing distribution of probabilities, which suggests the validity of the monitoring system and its potential for a severity analysis.

Ablation Study Training and validation loss curves are shown in Fig. A5 and show the importance of adopting a proper early stopping criteria. Three variants of the HRNN based on different fusion strategies, together with four variants of the SPEIs as input features are designed and used for comparison. Their results are given in Table A4. HRNN combining convolutional lateral connections with the last concatenation achieves the best results in Italy and Afghanistan, while no clear gain can be observed in Russia. The results of the SPEIs§ are close to that of SPEIs, suggesting extended ECVs historical records have less effect. Moreover, the results of SPEIs‡ are prominently inferior to other variants, which indicates that the variable standardization is the most essential step when computing the SPEIs.

Overall, these encouraging results demonstrate that HRNN is superior to the other models considered, either index-based or data-driven, which encourages developing further alternative hybrid models for drought monitoring.

Table 2: ROC-AUC scores for the different models and the three regions considered in this study

	SPEI 6	MLP	RNN	CMLP	DRNN	HRNN
Russia	0.740	0.711±0.002	0.764±0.009	0.702±0.006	0.717±0.008	**0.778±0.006**
Italy	0.797	0.871±0.001	0.895±0.009	0.917±0.011	0.935±0.007	**0.937±0.009**
Afghanistan	0.820	0.575±0.013	0.420±0.003	0.795±0.004	0.742±0.030	**0.825±0.004**

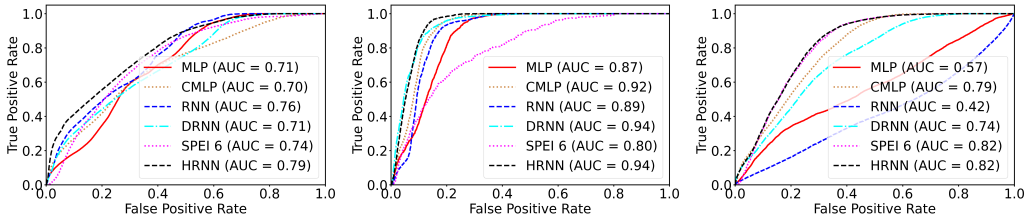

(a) Russia (b) Italy (c) Afghanistan

Figure 2: ROC Curves for the different models and the three regions considered in this study.

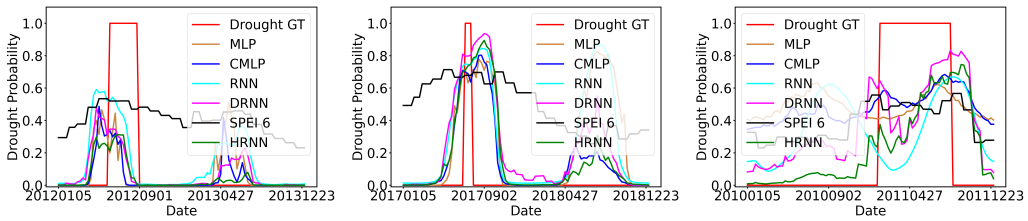

(a) Russia (b) Italy (c) Afghanistan

Figure 3: Detection signals through time for the different models and the three regions considered in this study.

5 Conclusions and Future Work

We proposed a hybrid recurrent neural network which, to our knowledge, constitutes the first hybrid machine learning model for drought monitoring. HRNN realizes the synergy between DL models and climatic indices and achieves superior performance over several representative drought events. An ablation study considering different fusion methods and indices demonstrated that convolutional lateral connections are optimal and the variable standardization step is essential for the computation of the SPEIs.

As future work, we plan to explore the fusion of SPEIs and ECVs within the inner loop of a RNN cell. This may improve the latent representations obtained for drought detection. Apart from assimilating knowledge through features, we also plan to explore the use of SPEIs for the regularization of DL models, as well as to learn the indices parameterization via end-to-end optimization.

Acknowledgments and Disclosure of Funding

M X Z appreciates the financial support from China Scholarship Council (CSC) through the State Scholarship Fund for Overseas Study (No. 202106710031). M A F T and G C V thank the support of the ERC Synergy Grant “Understanding and Modelling the Earth System with Machine Learning (USMILE)”, under Grant Agreement No 855187; the European Union’s Horizon 2020 research and innovation programme within the project ‘XAIDA: Extreme Events—Artificial Intelligence for Detection and Attribution’, under Grant Agreement No. 101003469; and the ESA AI4Science project "Multi-Hazards, Compounds and Cascade events: DeepExtremes", 2022-2024. The authors gratefully acknowledge the computer resources provided by the Juelich Supercomputing Centre (Project No. PRACE-DEV-2022D01-048) and Artemisa, funded by the ERDF and Comunitat Valenciana, as well as the technical support provided by the Instituto de Física Corpuscular, IFIC (CSIC-UV).

References

[1] Ashok K Mishra and Vijay P Singh. A review of drought concepts. *Journal of hydrology*, 391(1-2):202–216, 2010.

[2] Vincent Gitz, Alexandre Meybeck, L Lipper, C De Young, and S Braatz. Climate change and food security: risks and responses. *Food and Agriculture Organization of the United Nations (FAO) Report*, 110:2–4, 2016.

[3] Heidi Kreibich, Anne F Van Loon, Kai Schröter, Philip J Ward, Maurizio Mazzoleni, Nivedita Sairam, Guta Wakbulcho Abeshu, Svetlana Agafonova, Amir AghaKouchak, Hafzullah Aksoy, et al. The challenge of unprecedented floods and droughts in risk management. *Nature*, pages 1–7, 2022.

[4] Wayne C Palmer. *Meteorological drought*, volume 30. US Department of Commerce, Weather Bureau, 1965.

[5] Thomas B McKee, Nolan J Doesken, John Kleist, et al. The relationship of drought frequency and duration to time scales. In *Proceedings of the 8th Conference on Applied Climatology*, volume 17, pages 179–183. Boston, MA, USA, 1993.

[6] Sergio M Vicente-Serrano, Santiago Beguería, and Juan I López-Moreno. A multiscalar drought index sensitive to global warming: the standardized precipitation evapotranspiration index. *Journal of climate*, 23:1696–1718, 2010.

[7] Tayyebeh Mesbahzadeh, Maryam Mirakbari, Mohsen Mohseni Saravi, Farshad Soleimani Sardoo, and Mario M Miglietta. Meteorological drought analysis using copula theory and drought indicators under climate change scenarios (rcp). *Meteorological Applications*, 27(1):e1856, 2020.

[8] Vujica M Yevjevich. *Objective approach to definitions and investigations of continental hydrologic droughts, An*. PhD thesis, Colorado State University. Libraries, 1967.

[9] Khaled Hazaymeh and Quazi K Hassan. Remote sensing of agricultural drought monitoring: A state of art review. *AIMS Environmental Science*, 3(4):604–630, 2016.

[10] Baoqing Zhang, Amir AghaKouchak, Yuting Yang, Jiahua Wei, and Guangqian Wang. A water-energy balance approach for multi-category drought assessment across globally diverse hydrological basins. *Agricultural and forest meteorology*, 264:247–265, 2019.

[11] Foyez Ahmed Prodhan, Jiahua Zhang, Shaikh Shamim Hasan, Til Prasad Pangali Sharma, and Hasiba Pervin Mohana. A review of machine learning methods for drought hazard monitoring and forecasting: Current research trends, challenges, and future research directions. *Environmental Modelling & Software*, page 105327, 2022.

[12] E Fadaei-Kermani, GA Barani, and M Ghaeini-Hessaroeyeh. Drought monitoring and prediction using k-nearest neighbor algorithm. *Journal of AI and data mining*, 5(2):319–325, 2017.

[13] A Belayneh, J Adamowski, B Khalil, and J Quilty. Coupling machine learning methods with wavelet transforms and the bootstrap and boosting ensemble approaches for drought prediction. *Atmospheric research*, 172:37–47, 2016.

[14] Puyu Feng, Bin Wang, De Li Liu, and Qiang Yu. Machine learning-based integration of remotely-sensed drought factors can improve the estimation of agricultural drought in south-eastern australia. *Agricultural Systems*, 173:303–316, 2019.

[15] Runping Shen, Anqi Huang, Bolun Li, and Jia Guo. Construction of a drought monitoring model using deep learning based on multi-source remote sensing data. *International Journal of Applied Earth Observation and Geoinformation*, 79:48–57, 2019.

[16] Abhirup Dikshit, Biswajeet Pradhan, and Alfredo Huete. An improved spei drought forecasting approach using the long short-term memory neural network. *Journal of environmental management*, 283:111979, 2021.

[17] María González-Calabuig, Jordi Cortés-Andrés, Miguel-Ángel Fernández-Torres, and Gustau Camps-Valls. Recent advances in deep learning for spatio-temporal drought monitoring, forecasting and model understanding. *EGU22*, (EGU22-11872), 2022.

[18] Markus Reichstein, Gustau Camps-Valls, Bjorn Stevens, Martin Jung, Joachim Denzler, Nuno Carvalhais, et al. Deep learning and process understanding for data-driven earth system science. *Nature*, 566(7743):195–204, 2019.

[19] Valentina Zantedeschi, Daniele De Martini, Catherine Tong, Christian Schroeder de Witt, Alfredo Kalaitzis, Matthew Chantry, and Duncan Watson-Parris. Towards data-driven physics-informed global precipitation forecasting from satellite imagery. In *Proceedings of the AI for Earth Sciences Workshop at NeurIPS*, 2020.

[20] Laith J Abu-Raddad, Hiam Chemaitelly, Houssein H Ayoub, Patrick Tang, Peter Coyle, Mohammad R Hasan, Hadi M Yassine, Fatiha M Benslimane, Hebah A Al-Khatib, Zaina Al-Kanaani, et al. Relative infectiousness of sars-cov-2 vaccine breakthrough infections, reinfections, and primary infections. *Nature communications*, 13(1):1–11, 2022.

[21] Jun Li, Zhaocong Wu, Qinghong Sheng, Bo Wang, Zhongwen Hu, Shaobo Zheng, Gustau Camps-Valls, and Matthieu Molinier. A hybrid generative adversarial network for weakly-supervised cloud detection in multispectral images. *Remote Sensing of Environment*, 280:113197, 2022.

[22] Jordi Cortés-Andrés, Gustau Camps-Valls, Sebastian Sippel, Enikő Székely, Dino Sejdinovic, Emiliano Diaz, Adrián Pérez-Suay, Zhu Li, Miguel Mahecha, and Markus Reichstein. Physics-aware nonparametric regression models for earth data analysis. *Environmental Research Letters*, 17(5):054034, 2022.

[23] Miguel D Mahecha, Fabian Gans, Gunnar Brandt, Rune Christiansen, Sarah E Cornell, Normann Fomferra, Guido Kraemer, Jonas Peters, Paul Bodesheim, Gustau Camps-Valls, et al. Earth system data cubes unravel global multivariate dynamics. *Earth System Dynamics*, 11(1):201–234, 2020.

[24] S Beguería, B Latorre, F Reig, and SM Vicente-Serrano. sbegueria/speibase: Version 2.5. 1. *Glob. SPEI Database*, 2017.

[25] D Guha-Sapir, R Below, and PH Hoyois. Em-dat: International disaster database. université catholique de louvain, brussels, belgium, 2015.

[26] Julia Gottfriedsen, Max Berrendorf, Pierre Gentine, Markus Reichstein, Katja Weigel, Birgit Hassler, and Veronika Eyring. On the generalization of agricultural drought classification from climate data. *arXiv preprint arXiv:2111.15452*, 2021.

[27] Christoph Feichtenhofer, Haoqi Fan, Jitendra Malik, and Kaiming He. Slowfast networks for video recognition. In *Proceedings of the IEEE/CVF international conference on computer vision*, pages 6202–6211, 2019.

[28] Adam Paszke, Sam Gross, Francisco Massa, Adam Lerer, James Bradbury, Gregory Chanan, Trevor Killeen, Zeming Lin, Natalia Gimelshein, Luca Antiga, et al. Pytorch: An imperative style, high-performance deep learning library. *Advances in neural information processing systems*, 32, 2019.

[29] Diederik P Kingma and Jimmy Ba. Adam: A method for stochastic optimization. *arXiv preprint arXiv:1412.6980*, 2014.

Appendix

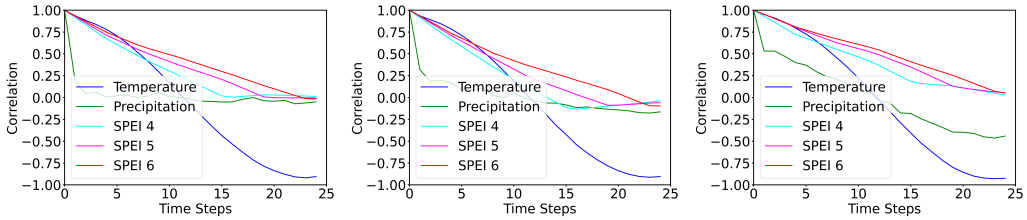

(a) Russia (b) Italy (c) Afghanistan

Figure A1: Time-lagged Spearman autocorrelation given input features (ECVs, SPEIs), averaged for all spatial locations.

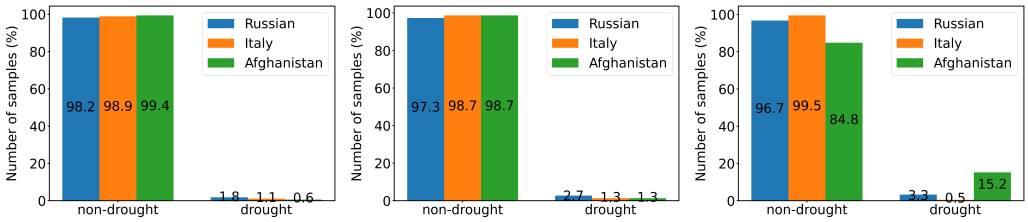

(a) Training (b) Validation (c) Test

Figure A2: Drought label distributions of the training, validation, and test dataset.

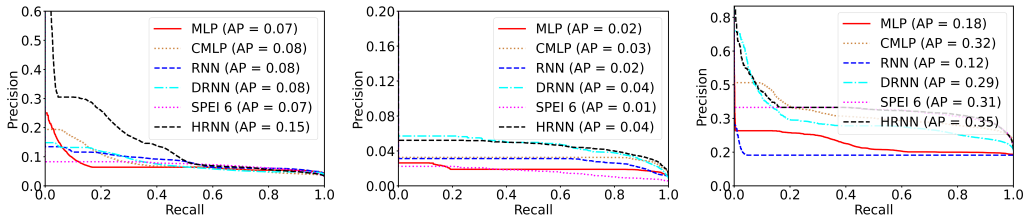

(a) Russia (b) Italy (c) Afghanistan

Figure A3: PR curves for the different models and the three regions considered in this study.

Table A1: Regions and drought events considered for the experiments

	Geospatial coordinates (NSWE)	Drought events
Russia	59.0°N, 43.0°S, 30.0°W, 64.0°E	Apr.−Aug. 2010; June−Aug. 2012
Italy	48.0°N, 35.0°S, 6.0°W, 19.0°E	June−Oct. 2012; July 2017
Afghanistan	38.0°N, 32.0°S, 63.0°W, 70.0°E	Oct. 2008; Jan.−Aug. 2011

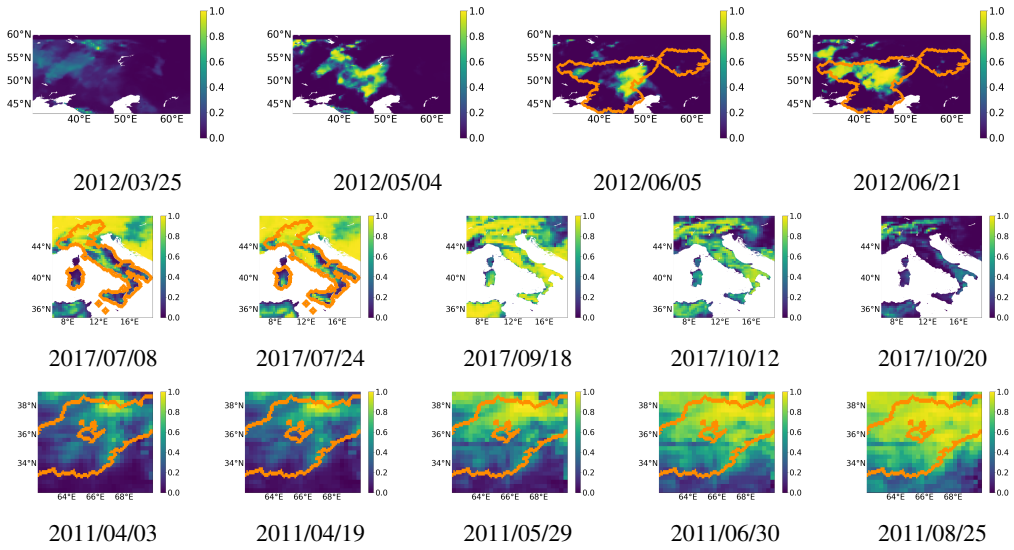

Figure A4: Drought monitoring maps obtained by HRNN over Russia (top row), Italy (middle row), and Afghanistan (bottom row), considered for the experiments. The subtitles are corresponding dates.

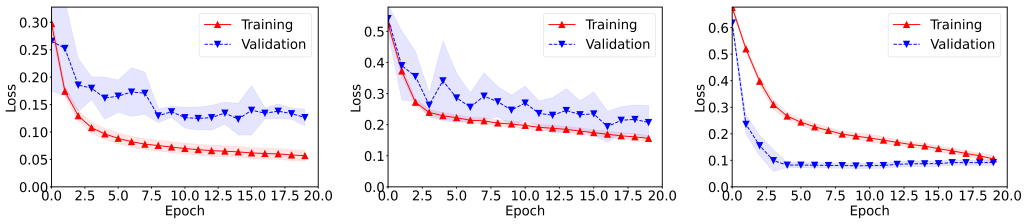

(a) Russia (b) Italy (c) Afghanistan

Figure A5: Loss curves obtained during the training stage of the HRNN proposed for the three regions considered. The shaded area shows the standard deviation for 10 independent executions.

Table A2: Hyperparameters of the DL models considered in this study

	MLP	RNN	CMLP	DRNN	HRNN
Activation	ReLU	Tanh	ReLU	Tanh	Tanh
Batch Norm	False	False	False	False	False (except in the LCs)
Dropout	0.5	0.5	0.5	0.5	0.5
Dual Branch	False	False	False	True	True
Fusion Method	-	-	Concat	Concat	LCs & Concat
Hidden Size	128	128	128	128	128
Including SPEIs	False	False	True	True	True
Layer Number	4	3	4	3	3
Batch Size	4096	4096	4096	4096	4096
Early Stop Patience	5	5	5	5	5
Epoch	20	20	20	20	20
Learning Rate	0.001	0.001	0.001	0.001	0.001

Table A3: Macro F1 and PR-AUC scores obtained for the different models and the three regions considered in this study

	SPEI 6	MLP	RNN	CMLP	DRNN	HRNN
1) Russia						
Macro F1	0.131	0.105±0.005	0.156±0.009	0.137±0.005	0.167±0.038	**0.230±0.015**
PR-AUC	0.066	0.069±0.003	0.083±0.004	0.080±0.001	0.089±0.018	**0.145±0.010**
2) Italy						
Macro F1	0.017	0.037±0.001	0.047±0.002	0.054±0.004	0.060±0.003	**0.066±0.005**
PR-AUC	0.015	0.018±0.000	0.023±0.005	0.030±0.005	**0.043±0.006**	0.041±0.009
3) Afghanistan						
Macro F1	0.365	0.246±0.002	0.162±0.004	**0.405±0.005**	0.354±0.024	0.377±0.013
PR-AUC	0.307	0.184±0.002	0.121±0.001	0.315±0.003	0.287±0.016	**0.348±0.002**

Table A4: Ablation study based on different HRNN and SPEIs variants, considering the three regions in this study

	HRNN	HRNN†	HRNN‡	HRNN§	SPIs	SPEIs†	SPEIs‡	SPEIs§
1) Russia								
Macro F1	0.230±0.015	0.240±0.014	0.242±0.010	0.215±0.020	0.158±0.023	0.213±0.027	0.098±0.028	0.233±0.020
PR-AUC	0.145±0.010	0.143±0.017	0.152±0.021	0.121±0.022	0.110±0.016	0.144±0.015	0.068±0.011	0.152±0.022
ROC-AUC	0.778±0.006	0.715±0.022	0.825±0.025	0.813±0.010	0.773±0.024	0.810±0.030	0.667±0.039	0.800±0.031
2) Italy								
Macro F1	0.066±0.005	0.064±0.004	0.045±0.003	0.059±0.005	0.069±0.002	0.066±0.003	0.036±0.004	0.071±0.004
PR-AUC	0.041±0.009	0.038±0.005	0.050±0.005	0.044±0.011	0.049±0.006	0.047±0.008	0.020±0.003	0.053±0.014
ROC-AUC	0.937±0.009	0.932±0.007	0.944±0.005	0.938±0.005	0.938±0.006	0.938±0.008	0.862±0.013	0.940±0.008
3) Afghanistan								
Macro F1	0.377±0.013	0.287±0.009	0.336±0.021	0.317±0.008	0.373±0.040	0.359±0.056	0.083±0.003	0.371±0.018
PR-AUC	0.348±0.002	0.285±0.002	0.265±0.011	0.263±0.005	0.402±0.037	0.327±0.034	0.128±0.002	0.364±0.007
ROC-AUC	0.825±0.004	0.771±0.002	0.716±0.020	0.703±0.013	0.823±0.037	0.795±0.045	0.445±0.004	0.807±0.010

HRNN variants: 1) HRNN without the last concatenation (HRNN†); 2) HRNN using reshaping lateral connections (HRNN‡); 3) HRNN using sampling lateral connections (HRNN§). SPEIs variants: 1) SPI index, based solely on precipitation; 2) SPEIs without latitude and month information within the PET estimation (SPEIs†); 3) SPEIs without the variable standardization based on probability distribution models, but instead using basic standardization (SPEIs‡); 4) SPEIs using extended ECVs historical records (SPEIs§).